

# Membrane Fouling in Dead-end Microfiltration of Yeast Suspensions

CRISTIANA LUMINITA GIJIU, ROMULUS DIMA\*, RALUCA DANIELA ISOPESCU

University Politehnica of Bucharest, Faculty of Applied Chemistry and Material Science, Chemical Engineering, Department, 1-7 Polizu Str., 011061, Bucharest, Romania

*Dead-end microfiltration of bakery yeast suspensions for 1, 5, 10 and 23 g/L were carried out in a batch membrane cell. The objective of this work was to identify which fouling mechanism is prevailing during the separation. The fouling mechanism was analyzed in terms of Hermia relation [4] and by a combined model. It was found that combined complete pore blockage-caking filtration model was the most useful because it was able to provide good fits of experimental data sets.*

*Keywords: membrane, dead-end microfiltration, fouling mechanism, yeast suspension*

Membrane filtration is an important process for separation of particulate matter and colloids from liquid suspension in many fields of engineering and applied science [1], but the membrane fouling is a major obstacle to the widespread use of this technology. Severe fouling requires cleaning or membrane replacement and this increase the operating costs.

The study of membranes fouling is at least as old as the study of membrane processes, but it seems that the last 20 years mark the beginning on an increased interest for this subject.

Membrane fouling is a process resulting in loss of performance of a membrane due to the deposition of suspended or dissolved substances on its external surfaces, at its pore openings or within its pores [2]. The phenomenon can cause important flux decline, as the effect of membrane resistance increases, and affects the quality of permeate.

For porous membrane the active area is the total area of the pores and hence most fouling mechanisms are related to a reduction in the number of active pores. Based on this, four models [3] are generally used to describe fouling (fig. 1).

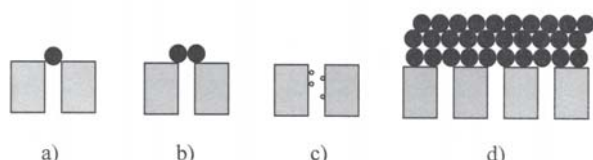


Fig. 1. Fouling mechanisms of porous membrane: a) complete pore blocking; b) partial pore blocking; c) standard pore blocking (pore constriction); d) cake filtration

Pore blockage increases the membrane resistance, while cake formation creates an additional layer of resistance to permeate flow. The fouling depends on the nature of the membrane and of the particle, the characteristics of the feed (pH, ionic strength) and the operating conditions (temperature, pressure, flow conditions).

During the process of membrane filtration the reduction of permeate flux is determined, from case to case, by different causes: the pore blocking, the polarization of the concentration and the formation of a precipitation layer.

For dead-end filtration at constant trans-membrane pressure and each fouling mechanism mentioned above, the dependence of area (A)/resistance (R) to filtration of specific volume of permeate  $v$  can be described by the following relationships [3,4]:

- complete pore blocking mechanism:

$$\frac{A}{A_0} = 1 - \frac{k_{cb} v}{J_0} \quad (1)$$

- partial pore blocking mechanism:  $\frac{A}{A_0} = \exp(-k_{pb} v)$  (2)

- standard pore blocking mechanism:  $\frac{R}{R_0} = \left(1 - \frac{k_{sb} v}{2}\right)^{-2}$  (3)

- cake filtration:  $\frac{R}{R_0} = (1 + 2k_{cf} J_0^2 \tau)^{0.5}$  (4)

Specific volume permeate can be calculated as a function of time by relations (5-8):

- complete pore blocking mechanism:

$$v = \frac{J_0}{k_{cb}} [1 - \exp(-k_{cb} \tau)] \quad (5)$$

- partial pore blocking mechanism:  $v = \frac{1}{k_{pb}} \ln(1 + k_{pb} J_0 \tau)$  (6)

- standard pore blocking mechanism:  $v = \left(\frac{1}{J_0 \tau} + \frac{k_{sb}}{2}\right)^{-1}$  (7)

- cake filtration:  $v = \frac{1}{k_{cf} J_0} \left[ (1 + 2k_{cf} J_0^2 \tau)^{0.5} - 1 \right]$  (8)

All of the classical models flux decline for dead-end filtration at constant pressure could be described by a single mathematical expression [4]:

$$\frac{d^2 \tau}{dV^2} = k \left( \frac{d\tau}{dV} \right)^n \quad (9)$$

where  $n$  is an exponent who depends on the fouling model ( $n = 0$  for cake filtration,  $n = 1$  for intermediate blockage,  $n = 3/2$  for pore constriction,  $n = 2$  for complete pore blockage).

Each of these mechanisms have been used individually to explain experimental results [5,6]. Although all these fouling models provide a mechanistic description for the fouling process, significant discrepancies between the flux decline data and model predictions are often observed. Many studies have shown a transition in fouling mechanism during the filtration process. For example, in [7] is shown that a plot of total resistance as a function of time is concave up when  $n > 1$  and is concave down when  $n \leq 1$ . Bowen et al. [8] obtained similar results using analysis based directly on eq. (9). In this case, the filtrate flux data at early times yielded an exponent of  $n \approx 2$  on a plot of  $d^2 \tau / dV^2$  versus  $d\tau / dV$  consistent with a pore blockage mechanism. The data at longer times suggested a cake filtration model, with  $n$  approaching zero and in some cases

\* email: r\_dima@chim.upb.ro; Tel.: 0741215621

attaining a negative value. These experimental studies provide evidence for a transition in fouling mechanism.

The first model that used two-stage mechanism (pore blockage and cake filtration) which describes membrane fouling was developed by [9]. Recently other three theoretical models [10-12], validated by experimental results, were developed as combined fouling mechanisms.

Development of effective methods to control fouling is determined by understanding of fouling mechanism and the influence of process parameters on this phenomenon. A synthesis about the various methods to reduce or, where possible, to eliminate fouling in microfiltration and ultrafiltration separations is presented in [13].

The objective of this work was to identify which fouling mechanism is prevailing during the microfiltration of yeast suspensions. In another work [14] the fouling determined by *Pseudomonas Aeruginosa* cells from the culture broth was studied.

### Experimental part

In this paper dead-end microfiltration of synthetically prepared aqueous yeast solutions was carried out using cellulose nitrate membrane with 0.2 $\mu$ m pore size dimensions, from Sartorius. Pure yeast cells using a concentration 1, 5, 10 and 23 g/L were suspended in distilled water. Yeast suspensions contain particles in the range 1-3 $\mu$ m determined by optical microscopy investigation (magnitude 100X). The images were captured by a video camera and processed using a software that counts the particles and provides the equivalent diameter and the shape factors. These data were treated by common statistical methods and represented as histograms (fig.2).

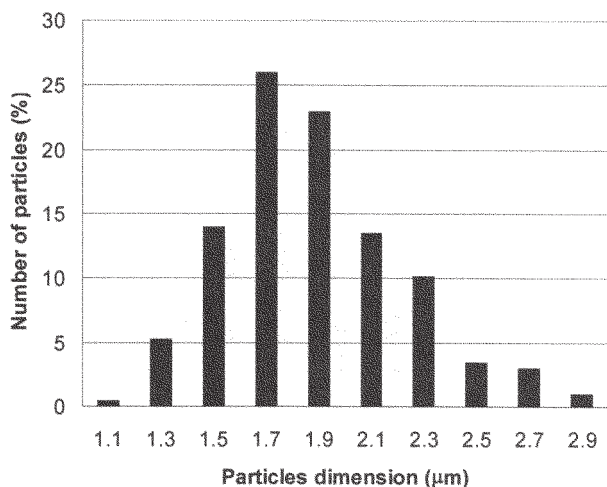


Fig. 2 – Distribution of yeast particle size

Dead-end microfiltration module, depicted in figure 3, was purchased from Millipore, with 300 cm<sup>3</sup> volume cell and 39.6 cm<sup>2</sup> membrane area. The pressure in the cell, adjusted by manually operated valve, was measured using a pressure gauge. The permeate flux was measured volumetrically.

For nitrate cellulose membrane was initially determined the permeability for distilled water in the pressure range 0.6-2 bar.

Dead-end experiments of aqueous yeast solutions were carried at room temperature (20-23°C) and for 1 bar trans-membrane pressure, with moderate agitation speed. After each run, the permeability of membrane was again measured, after its cleaning and rinsing with distilled water, and this value of permeate flux was considered as initial flux ( $J_0$ ) for another experiment.

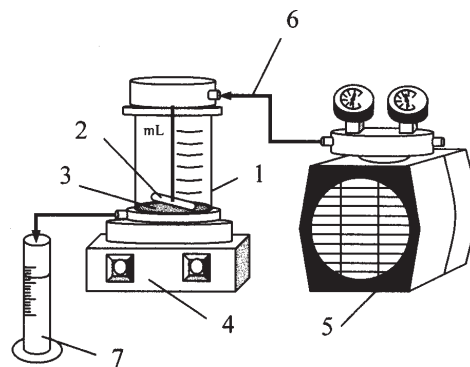


Fig. 3 – Schematic diagram of dead-end filtration apparatus: 1- Amicon cell; 2 - stirrer bar; 3 - magnetic stirrer; 4 - Millipore pressure/vacuum pump; 5 - compressed air line; 6 - permeate line; 7 - permeate vessel

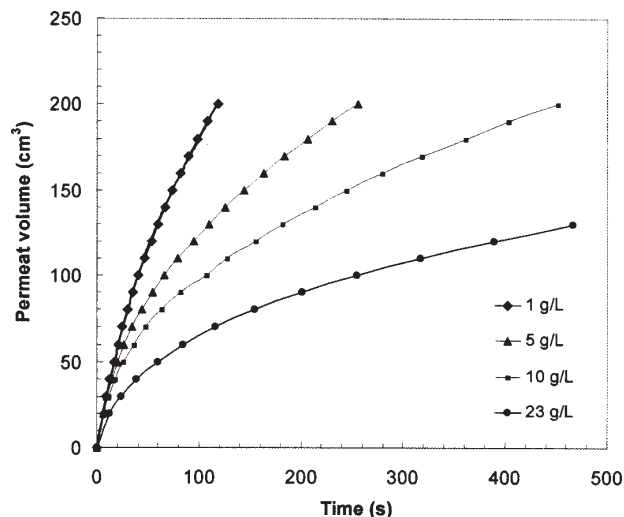


Fig. 4. Experimental data trials for yeast suspension

### Results and discussions

Experimental trials for yeast suspension shows a nonlinear relationship between permeate volume versus time (fig. 4) and thus a variable permeate flux, result which indicates an (important) fouling level of membrane. Relation (9) was used to identify the fouling mode. The evaluation of the value of parameter  $n$  enables the identification of the controlling specific mechanism. The procedure followed is presented below:

- the relationship (polynomial type) between time and permeate volume was drawn;
- the first derivative of polynomial ( $d\tau / dV$ ) was plotted against the permeate volume and another polynomial regression for correlation  $d\tau / dV = f(V)$  was derived;
- the second derivative of the polynomial ( $\frac{d^2\tau}{dV^2}$ ) was

calculated, the value  $\ln \left( \frac{d^2\tau}{dV^2} \right)$  was plotted against  $\ln(d\tau / dV)$  to determinate the  $n$  value (relation 9) from the slope of the curve which characterises each fouling mechanisms.

Following the procedure described,  $n > 0$  proved to correspond for each experiment. At the same time after each run a cake layer was observed on the membrane surface. For this reason a combined mechanism complete pore blocking - cake filtration (CB-CF) was considered. The standard pore blocking mechanism was excluded because yeast particle sizes are larger than membrane pores (fig. 1). In accordance with this model, during the initial stage

**Table 1**  
THE VALUES OF PARAMETERS AND ERROR FIT FOR CB-CF AND PB-CF MODEL

Yeast concentration (g/L)	CB-CF model			PB-CF model		
	$k_{cb}$ ( $s^{-1}$ )	$k_{cf} \cdot 10^{-5}$ ( $s \cdot m^{-2}$ )	$\sigma(k_{cb}, k_{cf}) \cdot 10^6$	$k_{pb}$ ( $s^{-1}$ )	$k_{cf} \cdot 10^{-5}$ ( $s \cdot m^{-2}$ )	$\sigma(k_{pb}, k_{cf}) \cdot 10^6$
1	$1.453 \cdot 10^{-9}$	0.711	27.44	25.8	0.16	176.4
5	$6.635 \cdot 10^{-3}$	1.244	0.8	34.3	0.26	108.7
10	$1 \cdot 10^{-2}$	2.144	4.07	46.3	0.32	154.7
23	$1.1 \cdot 10^{-2}$	4.63	0.17	47.9	0.29	406.1

of membrane filtration the yeast particles seal the pore entrances. As time progressed, the particles accumulate at the membrane surface in a permeable cake of increasing thickness. The combined model takes into account the loss of area filtration determined by pore blockage and the increase in resistance generated by the cake filtration model.

The permeate flow rate at the start of separation ( $Q_0$ ) and at  $\tau$  moment ( $Q$ ) can be described by Darcy relation:

$$Q_0 = \frac{A_0 \Delta p}{\eta R_0} \quad \text{and} \quad Q = \frac{A \Delta p}{\eta R}$$

from which:

$$\frac{Q}{Q_0} = \frac{AR_0}{A_0 R} \quad (10)$$

If the flux is defined by the relation:

$$J = \frac{Q}{A_m}$$

a similar relation is obtained for the corresponding flux ratio:

$$\frac{J}{J_0} = \frac{A}{A_0} \frac{R_0}{R} \quad (11)$$

If a combined fouling model is considered (cake filtration and complete pore blockage), relations (1) and (4) can be used for the two ratios from equation (11).

$$\frac{J}{J_0} = \left( 1 - \frac{k_{cb}}{J_0} v \right) \left( 1 + 2k_{cf} J_0^2 \tau \right)^{-0.5}$$

or in a similar form:

$$J = \frac{dv}{d\tau} = J_0 \left( 1 - \frac{k_{cb}}{J_0} v \right) \left( 1 + 2k_{cf} J_0^2 \tau \right)^{-0.5} \quad (12)$$

The solving of differential equation (12) gives the specific permeate volume versus time:

$$v = \frac{J_0}{k_{cb}} \left[ 1 - \exp \left( - \frac{k_{cb}}{k_{cf} J_0^2} \left( \sqrt{1 + 2k_{cf} J_0^2 \tau} - 1 \right) \right) \right] \quad (13)$$

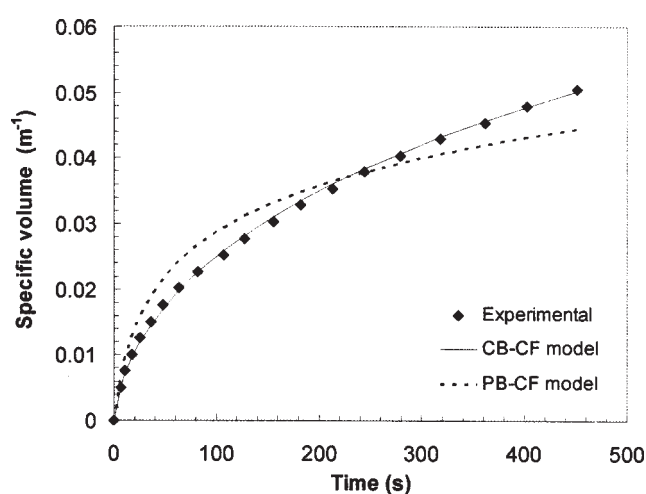


Fig. 5. Experimental data and combined models predictions

By a similar procedure is possible to obtain the relation of specific volume versus time for a combined partial pore blocking-cake filtration (PB-CF) model (eq. 14):

$$v = \frac{1}{k_{pb}} \ln \left[ 1 + \frac{k_{pb}}{k_{cf} J_0} \left( \left( 1 + 2k_{cf} J_0^2 \tau \right)^{0.5} - 1 \right) \right] \quad (14)$$

To verify models predictions it is necessary to calculate the values of constants  $k$  from equations (13) or (14) which better fits the experimental data. For each set, numerical calculations were performed with Mathcad by minimizing the sum of squared residuals (named  $\sigma(k_{cb}, k_{cf})$  or  $\sigma(k_{pb}, k_{cf})$  in table 1) between values of experimental specific permeate volume and the model prediction. The values obtained are presented in table 1.

The data and the model predictions for the yeast concentration in suspension  $c = 10$  g/L are presented in figure 5. The combined complete blocking-cake filtration model represents the best approximation of experimental data.

Similar results for the calculated parameters were obtained for the 1, 5 and 23 g/L yeast concentration. Similar with the case of 10 g/L yeast concentration, the best value for the objective function,  $\sigma(k_{cb}, k_{cf})$  corresponds to the CB-CF model (table 1).

On the basis of  $k_{cb}$  and  $k_{cf}$  values the contribution of complete pore blocking versus cake filtration can be evaluated. Both constants increase with the yeast concentration, but the  $k_{cf}$  parameter remains greatest, so that the cake filtration is probably the main fouling mechanism.

### Conclusions

The dead-end microfiltration of bakery yeast aqueous suspensions, synthetically prepared, with the concentration in the range 1-23 g/L was performed in a stirred cell using a nitrate cellulose membrane with 0.2 $\mu$ m pore size dimensions at 1 bar trans-membrane pressure.

The shape of the curves  $V = f(\tau)$  relieves the fouling phenomenon which increases with the yeast concentration. To identify the fouling mechanism, the Hermia relation was first tested. The value of the  $n$  parameter was in the range  $0 < n < 1$  for all experimental runs effectuated which denotes a combined mechanism. Because the dimensions of yeast particles were larger than membrane pore size diameter, a standard pore blockage was excluded.

For this reason a possible combined pore blocking-cake filtration model was used. The parameters of two possible models (complete or partial pore blockage coupled with cake filtration) were determined. The data fit gave better results for combined complete blocking-cake filtration than partial blocking-cake filtration model. As concerns the relative importance of the two mechanisms, the cake filtration is probably the main fouling mechanism.

### Nomenclature

$A$  – available membrane filtration area ( $m^2$ )  
 $A_0$  – initial membrane filtration area ( $m^2$ )  
 $A_m$  – effective membrane surface area ( $m^2$ )  
 $J$  – permeate flux ( $m \cdot s^{-1}$ )  
 $J_0$  – initial permeate flux ( $m \cdot s^{-1}$ )  
 $k$  – constant (rel. 9)

$k_{cb}$  – complete blocking constant ( $s^{-1}$ )  
 $k_{cf}$  – cake filtration constant ( $s \cdot m^{-2}$ )  
 $k_{pb}$  – partial blocking constant ( $m^{-1}$ )  
 $k_{sb}$  – standard blocking constant ( $m^{-1}$ )  
 $R$  – resistance to filtration ( $m^{-1}$ )  
 $R_0$  – initial membrane resistance ( $m^{-1}$ )  
 $V$  – volume permeate ( $m^3$ )  
 $v$  – specific volume permeate ( $m^3 \cdot m^{-2}$ )  
 $Q$  – permeate flow rate ( $m^3 \cdot s$ )  
 $Q_0$  – initial permeate flow rate ( $m^3 \cdot s$ )  
 $\Delta p$  – trans-membrane pressure (Pa)  
 $\tau$  – time (s)

### References

- SCOTT, K., Handbook of Industrial Membranes, Elsevier Advanced Technology, 1998, Oxford, UK.
- KOROS, W.J., MA Y.H., SHIMIDZU, T., J. Membr. Sci., **120**, 1996, p.149.
- GRACE, H.P., AIChEJ, **2**, 1956, p.307.
- HERMIA, J., Trans. Inst. Chem. Eng, **60**, 1982, p. 183.
- HLAVACEK, M., BOUCHET, F., J. Membr. Sci, **82**, 1993, p. 285.
- KELLY, E.M., DAVIS, R.H., J. Membr. Sci, **107**, 1995, p. 115.
- TRACEY, E.M., DAVIS, R.H., J. Colloid Interface Sci., **167**, 1994, p.104.
- BOWEN, W.R., CALVO, J. I., HERNANDEZ, A., J. Membr. Sci, **101**, 1995, p. 153
- HO, C.C., ZYDNEY, A.L., J. Colloid Interface Sci., **232**, 2000, p.389.
- DUCLOS-ORSELO, C., LI, W., HO, C.C., J. Membr. Sci, **280**, 2006, p. 856.
- GRENIER, A., MEIRELES, M., AIMAR, P., CARVIN, P., Chem. Eng. Res. Des., **86**, 2008, p. 1281.
- BOLTON, G., LaCASSE, D., KURIYEL, R., J. Membr. Sci., **277**, 1996, p.75.
- HILAL, N., OGUNBIYI, O.O., MILES, N.J., NIGMATULLIN, R., Sep. Sci. Tech., **40**, 2005, p.1957.
- UNGUREANU, C., DIMA, R., ONU, A., MIHALCEA, A., Rev. Chim. (Bucharest), **60**, no. 1, 2009, p. 48.

Manuscript received: 8.06.2011